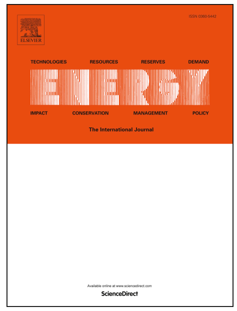

Effects of gas components, reservoir property and pore structure of shale gas reservoir on the competitive adsorption behavior of CO_2 and CH_4

Weidong Xie, Meng Wang, Si Chen, Veerle Vandeginste, Zhenghong Yu, Hua Wang

PII: S0360-5442(22)01145-8

DOI: https://doi.org/10.1016/j.energy.2022.124242

Reference: EGY 124242

To appear in: *Energy*

Received Date: 17 December 2021

Revised Date: 1 May 2022

Accepted Date: 10 May 2022

Experimental design and data analysis, Weidong Xie, Zhenghong Yu, and Hua Wang. Writing and revision, Weidong Xie, Meng Wang, Si Chen, and Veerle Vandeginste.

Effects of gas components, reservoir property and pore structure of shale gas reservoir on the competitive adsorption behavior of CO_2 and CH_4

Weidong Xie [a], Meng Wang [b*], Si Chen [a*], Veerle Vandeginste [c], Zhenghong Yu [a], Hua Wang [a]

[a] School of Earth Resources, China University of Geosciences, Wuhan 430074, China;

[b] School of Resources and Geosciences, China University of Mining and Technology, Xuzhou 221008, China;

[c] KU Leuven, Campus Bruges, Department of Materials Engineering, B-8200 Bruges, Belgium.

* Email: wangm@cumt.edu.cn

* Email: sichen720@hotmail.com

Abstract

CO_2 injection into shale gas reservoirs is deemed as a potential scheme to enhance CH_4 recovery and achieve the ambition of carbon neutral. The insufficient research of binary gas competitive adsorption behavior at in-situ conditions of shale gas reservoirs, and the coupling control of gas components, shale properties, and pore structure on CO_2 adsorption affinity limit its general application. Therefore, the competitive adsorption behavior of CO_2 and CH_4 at in-situ conditions is simulated using high-pressure multi-component adsorption experiments, and the effects of binary gas components, shale properties and pore structure on CO_2 adsorption affinity are discussed. Subsequently, the mathematical and geological models of CO_2 injection into Longmaxi shale gas reservoir enhancing CH_4 recovery and achieving carbon sequestration are established based on experimental parameters and reservoir geological parameters, and the feasibility and expectation benefits are discussed. The results exhibit that selectivity coefficient of CO_2 relative to CH_4 (Sc) decreases with higher CO_2 mole fraction, whereas it increases with higher total organic carbon content (TOC) and clay content. Both pore volume (PV) and specific surface area (SSA) have clear positive correlations with Sc. Overall, TOC is a crucial controlling factor of pore structure and adsorption capacity of shale, further, affects the adsorption affinity of CO_2. The injection of CO_2 into shale gas reservoir shows a promising application prospect in improving CH_4 recovery and carbon emission reduction in geological and mathematical models, and the leakage risk is low after CO_2 sequestration.

Keywords: adsorption affinity; binary gas components; reservoir property; pore structure; enhanced CH_4 recovery; CO_2 sequestration.

1 Introduction

The shale gas reservoir is characterized by low porosity and low permeability, and reservoir reconstruction is needed in the development process to improve gas production [1,4]. Although hydraulic fracturing effectively enhances gas recovery, it has not ever been permitted in several countries due to its disadvantages such as consumption of water resources, environmental pollution, and reservoir damage [5-8]. It is urgent to develop clean and efficient alternative techniques. In addition, Massive CO_2 emission has triggered sever environmental problems, in which global warming threatened the living environment of organisms [9-10]. In the context of the global carbon neutral ambition and the exploration of new exploitation techniques to enhance CH_4 recovery of shale gas reservoir, the injection of CO_2 into shale is a promising solution [1-3]. Shale gas reservoir is a potential sequestration space of CO_2 due to its huge volume and wide distribution. Besides, the high adsorption affinity of CO_2 can promote the desorption of the pre-adsorbed CH_4 to enhance gas recovery [2,11]. Previous exploitation experience learns that the initial shale gas production is determined by free gas, whereas the stable yield cycle is controlled by the adsorbed gas [4,12]. The purpose of CO_2 injection is to promote CH_4 desorption, yielding free CH_4 gas [3-4,12]. In this way, shale gas production can be improved in the stable production period by free gas, and the stable production cycle can be extended [11,13]. Additionally, CO_2 subsurface sequestration is achieved by the strong self-sealing ability of shale [14-15]. Many pure CH_4 or CO_2 adsorption experiments were conducted, and the studies generally concluded that the adsorption amount of CO_2 in shale is up to ten times higher than CH_4 [16-17]. Thus, the injection of CO_2 would occupy the adsorption sites of CH_4 (pre-adsorbed in the reservoir) and promote CH_4 desorption, which is the anticipated behavior and a prerequisite for CO_2 storage and to improve CH_4 recovery in shale gas reservoir [2,16].

Still, in real shale gas reservoirs, there are no pure but rather mixed gases after CO_2 injection [18,19]. Hence, pure CH_4 and CO_2 comparative adsorption is not sufficient to accurately, directly, and comprehensively represent the competitive adsorption behavior in practice. Accordingly, multi-component gas adsorption experiments were conducted to detect the competitive adsorption behavior of CH_4 and CO_2 [13,20-21]. The main experimental method includes low field nuclear magnetic resonance, isothermal adsorption instrument-mass spectrometry, and isothermal adsorption instrument-gas chromatography [22-24]. The results demonstrate that the adsorption amount and affinity of CO_2 is still significantly greater than CH_4 in the binary gas adsorption system in the shale matrix, and Sc decreases with higher experimental pressure [16,23-24]. Moreover, there is not only interaction between the gas and the shale matrix, but also interaction among gas molecules in the binary gas adsorption system [13,21]. However, previous studies were conducted with a maximum experimental pressure of less than 6 MPa, which does not reflect the conditions of real shale gas reservoirs [16,24]. The commercial shale gas reservoirs are buried more than 1000 m depth, and the corresponding hydrostatic pressure is over 10 MPa, or even exceeds 100 MPa for some deep reservoirs [25-27]. Furthermore, there are many studies on molecular simulation of high-pressure competitive adsorption, and the results suggest that the adsorption amount, affinity and priority of CO_2 were significantly higher than CH_4, but high-pressure experimental simulation of multi-component adsorption of CO_2 and CH_4 in shale is insufficient [28-30]. Hence, the reliability of these molecular simulation studies is limited because: (i) molecular simulation is based on a hypothetical adsorption theory and the ideal kerogen/clay mineral structure model. (ii) The shale matrix is not regarded as a whole, and the adsorption of gas on kerogen or clay minerals are discussed separately. (iii) The setting of adsorption parameters mostly refers to the experimental results of pure components adsorption, which ignores the interaction of CH_4 and CO_2 molecules and it is not representative for binary gas adsorption. (iv) The results of molecular simulation need to be mutually verified by physical experimental simulation corresponding to environmental conditions.

Therefore, high-pressure binary adsorption experiments are necessary for the simulation of CH_4 and CO_2 adsorption in the simulated shale gas reservoir conditions and to verify the molecular simulation results.

Additionally, the mixing of CH_4 and CO_2 is not uniform in shale gas reservoirs after CO_2 injection [11,18]. Hence, the gas injection ratio of CH_4 and CO_2 also has a significant impact on the competitive adsorption behavior [21,23]. The experimental and molecular simulation results suggest that the gas adsorption capacity in shale increases with higher CO_2 mole fraction in the binary gas adsorption system, whereas Sc decreases with higher CO_2 mole fraction [21,31-32]. However, the experimental simulation is mostly in low-pressure, and the setting range of the mixed gas ratio is relative narrow. Additionally, binary gas occurs in a shale matrix with various pore sizes after CO_2 injection [4,12]. The pores are divided into micropores (pore diameter is in the range of 0 - 2 nm), mesopores (2 - 50 nm), and macropores (> 50 nm) according to the classification scheme of International Union of Pure and Applied Chemistry [33]. The corresponding pore structure parameters (PV and SSA) control the occurrence space and adsorption sites [21,34]. Generally, PV is controlled by micropores and mesopores, and SSA is mainly controlled by micropores with a proportion greater than 90% [35-37]. Consequently, the role of micropores needs to be discussed in depth. Furthermore, micropores are divided into super-micropores (1.4 - 2 nm), micropores (0.7 - 1.4 nm), and ultra-micropores (< 0.7 nm) [33]. Currently, the influence of pore structure parameters of various pore sizes on CO_2 adsorption affinity relative to shale is poorly documented, and thus, this needs more detailed and in-depth discussion. Moreover, the accumulation space of shale gas is mainly provided by organic matter and clay minerals [38-40]. Consequently, the relationship between TOC, clay content, pore structure parameters, and Sc needs to be revealed.

Therefore, we have performed pure gas and binary gas adsorption experiments at 50 ℃ and pressure up to 20 MPa. To restore the in-situ environmental conditions of the real shale gas reservoirs as much as possible, the experimental temperature and pressure are set as the highest value of the adsorption instruments under the normal operating conditions. The excess adsorption amount (Vex) is corrected to absolute adsorption amount (Vabs) according to the results of adsorption experiments, and V_L and Sc values are calculated. The high-pressure isothermal adsorption experiments of binary gas are conducted to simulate the competitive adsorption process between CO_2 and CH_4 in the reservoir, and the evolution regularity of CO_2 adsorption affinity is discussed in different gas reservoirs by changing the components of feed gas (includes seven sets of CH_4 (100%), CH_4 (80%) +CO_2 (20%), CH_4 (60%) +CO_2 (40%), CH_4 (50%) +CO_2 (50%), CH_4 (40%) +CO_2 (60%), CH_4 (20%) +CO_2 (80%), and CO_2 (100%)). Low-temperature N_2 and CO_2 adsorption experiments are performed to obtain pore structure parameters of reservoir, and the influence of PV and SSA at different pore sizes on the competitive adsorption behaviors is discussed. Furthermore, coupling relationships of V_L and Sc versus binary gas composition, TOC, clay content, and pore structure parameters are discussed. Finally, the mathematical and geological models are established based on above experimental parameters and reservoir geological parameters of

Longmaxi shale in Sichuan Basin (sampling points), which aims to evaluate the feasibility, benefits, and safety of CO_2 subsurface sequestration and enhanced CH_4 recovery in deep shale gas reservoirs. Results of this examination are expected to further promote the research on competitive adsorption behavior and the controlling factors of multi-component gas in shale at high pressure, and they establish a reference for CO_2 injection into shale gas reservoirs to improve CH_4 recovery and carbon sequestration process.

2 Sample, experiment, and method

2.1 Sample and experiment

2.1.1 Sample collection and preparation

Samples in this examination are collected from the Longmaxi Formation of Lower Silurian, southern Sichuan Basin, which is a national demonstration area for the commercial exploitation of marine shale gas reservoirs. Five drilling core shale samples are from Well X in southern Sichuan Basin, and numbered XY-1 - XY-5 from the bottom to top, respectively. The samples are put into plastic bags after collection and sent to the laboratory immediately. Additionally, each sample is processed at specifications according to the subsequent experimental requirements. An aliquot of 5 g shale sample was ground to 100 - 200 mesh for TOC tests, 2 g shale sample ground to less than 200 mesh for X-ray diffractometer tests, 8 g shale sample ground to 40 - 60 mesh for low-temperature N_2 and CO_2 adsorption experiments, and 10 g shale sample ground to 80 - 100 mesh for pure gas and binary gas isothermal adsorption tests.

2.1.2 Tests of TOC, R_o, mineralogical composition, and pore structure parameters.

Before the isothermal adsorption experiments, the organic geochemical characteristics, mineralogical composition, and pore structure parameters of shale samples are tested. The TOC of five shale samples is obtained by using CS230SH carbon sulfur analyzer according to the standard GB/T 19145-2003 [41]. *R*o is observed by using DM4500P Polarizing microscope and QDI302 spectrophotometer according to the standards GB/T 6948-1998 and SY/T 5124-2010 [42-43]. The mineralogical composition is measured by using X'Pert MPD PRO X-ray diffractometer according to the standard SY/T 5163-2010 [44]. Pore structure parameters are measured by using low-temperature N_2 and CO_2 adsorption experiments (NOVA2000e automatic porosity and specific surface analyzer), the experimental process refers to the standard GB/T 7702.20-2008 [45]. According to the test accuracy of the two experiments, low temperature CO_2 adsorption test results are selected for pores in the range of 0 - 1.5 nm and low temperature N_2 adsorption results are selected for pores in the range of 1.5 - 50 nm. The results are presented in Tables 1 and 2.

Table 1 Organic geochemical parameters and mineralogical composition of shale samples

Sample ID	OGP (%)		Mineralogical composition (%)						RCOC (%)			
	TOC	R_o	Clay	Quartz	Feldspar	Carbonate	Siderite	Pyrite	Kaolinite	Chlorite	Mixed I/S	Illite
XY-1	3.78	3.19	24.13	32.47	24.9	17.13	0	1.38	8	14	0	78
XY-2	4.065	2.914	31.26	39.68	23.13	5.26	0.44	0.23	6	12	0	82
XY-3	3.15	2.8	27.54	31.41	23.43	16.95	0	0.67	6	12	0	82
XY-4	2.87	2.943	17.39	33.8	28.27	19.87	0	0.68	7	13	0	80

XY-5	2.52	2.726	20.11	34.78	29.49	14.32	0.62	0.67	7	11	4	78

Notes: OGP is organic geochemical parameters, RCOC is relative content of clay minerals.

Table 2 Micropore and mesopore structure parameters of five shale samples

Sample ID	PV (cm^3/g)						SSA (m^2/g)					
	0-0.7	0.7-1.4	1.4-2	0-2	2-50	0-50	0-0.7	0.7-1.4	1.4-2	0-2	2-50	0-50
XY-1	0.00293	0.00117	0.00039	0.00449	0.01300	0.01749	11.45	2.60	0.87	14.92	9.98	24.91
XY-2	0.00321	0.00202	0.00060	0.00584	0.01345	0.01929	13.08	4.26	1.23	18.57	9.93	28.51
XY-3	0.00230	0.00228	0.00069	0.00527	0.01200	0.01727	8.72	4.81	1.25	14.78	9.51	24.29
XY-4	0.00227	0.00154	0.00037	0.00418	0.01161	0.01578	9.00	3.23	0.72	12.95	8.71	21.66
XY-5	0.00220	0.00172	0.00041	0.00433	0.01120	0.01553	8.46	2.77	0.65	11.88	8.52	20.41

Notes: PV is pore volume, cm^3/g; SSA is specific surface area, m^2/g; "0-0.7" is pore size, nm.

2.1.3 Isotherm adsorption experiments

(1) Experimental instrument and experimental scheme

Binary gas isothermal adsorption instrument consists of gravimetric isothermal adsorption instrument and gas chromatograph, including three portions of quantitative gas mixing device (serve to feed gas ratio setting of CH_4 and CO_2), gas adsorption system (complete the adsorption behavior of CH_4 and CO_2 on shale matrix and the temperature control of adsorption system), and gas adsorption identification system (record the changes of sample weight, gas density, and concentration by magnetic suspension balance and gas chromatograph) (Fig. 1). Competitive adsorption experiments of mixed gas consist of two series. (i) Experiments on the change of mole fraction of CH_4 and CO_2 in the binary gas, containing seven gas ratios of CH_4 (100%), CH_4 (80%) +CO_2 (20%), CH_4 (60%) +CO_2 (40%), CH_4 (50%) +CO_2 (50%), CH_4 (40%) +CO_2 (60%), CH_4 (20%) +CO_2 (80%), and CO_2 (100%), which are conducted on sample XY-1. (ii) Binary gas adsorption experiments on the change of organic geochemical parameters, mineralogical composition, and pore structure parameters, containing five samples of XY-1, XY-2, XY-3, XY-4, and XY-5. The setting of feed gas composition refers to the results of (i), and CH_4 (60%) +CO_2 (40%) is selected because of its most significant change in gas mole fraction.

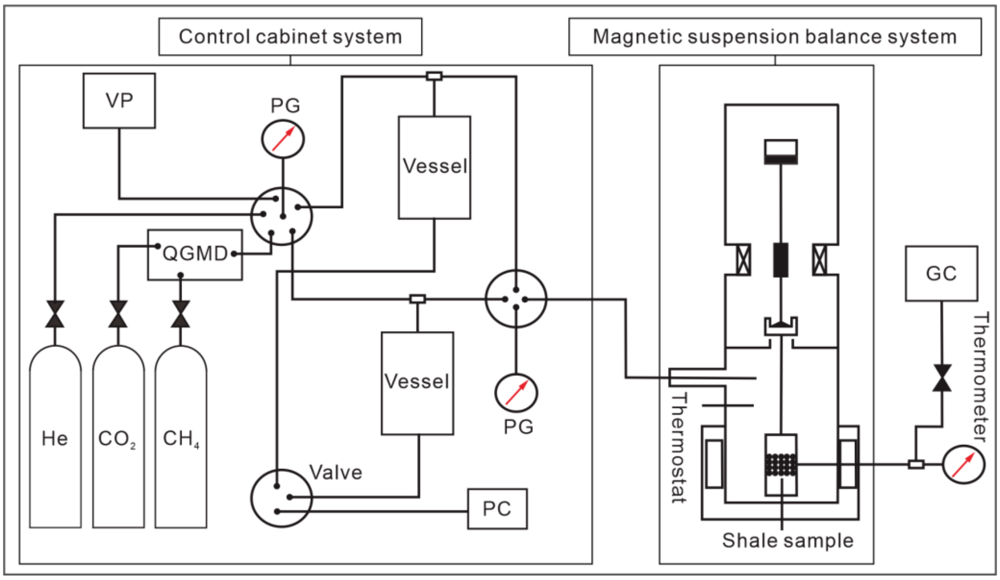

VP is vacuum pump, its limiting pressure is 100 MPa; PG is pressure gauge with an accuracy of ± 0.001 MPa; QGMD is quantitative gas mixing device, which severs the configuration of the mixed gas; GC is gas chromatograph, which is used to record the composition of the mixed gas in the adsorption system; PC is pressure controller with an accuracy of ± 0.001 MPa. Thermostat is a set of oil bath thermostatic system, which enables the control of experimental temperature with an accuracy of ± 0.1 ℃.

Fig. 1 Binary gas isothermal adsorption instrument

(2) Experimental procedure

Before the competitive adsorption experiments of binary gas, air tightness inspection, blank test, pretreatment test, and buoyancy test are carried out on the experimental device and shale samples, which provide the weight and volume of the sample cell and shale sample. Then, competitive adsorption experiments with different feed gas composition or shale samples are carried out first. CH_4 and CO_2 are injected into a quantitative gas mixing device, allowing a binary mixture with different mole fractions of CH_4 and CO_2. Adsorption experiments are performed according to the designed experimental pressure points. The first pressure point is set to vacuum (P < 1kPa). Adsorption equilibrium is considered when temperature change of the adsorption system is less than 0.2 ℃ and the duration maintained is more than two hours. Temperature, pressure, and balance readings are collected every two minutes during the experimental process. After reaching the equilibrium conditions, the average of the five recorded data after equilibrium is selected as the final reading, and then the mole fractions of CH_4 and CO_2 in the bulk phase are recorded by the gas chromatograph. Subsequently, competitive adsorption experiments of each experimental pressure point and experimental shale sample are performed in turn.

2.2 Calculation methods

2.2.1 Correction of absolute adsorption amount

The result directly measured in the adsorption experiments is the excess adsorption amount, which ignores the volume of the adsorption phase, resulting in a value lower than the real adsorption amount [46-47]. This can be corrected to the absolute adsorption amount by Eq. 1 to characterize the real adsorption amount (absolute adsorption amount) of adsorbent for adsorbate [48-49].

$$\mathrm{Vabs} = \mathrm{Vex} / (1 - \rho_g/\rho_a) \tag{1}$$

For binary gas adsorption (Eqs. 2 and 3):

$$\rho_g = x_1\rho_{g1} + x_2\rho_{g2} \tag{2}$$

$$\rho_a = y_1\rho_{a1} + y_2\rho_{a2} \tag{3}$$

Vabs is the absolute adsorption amount, cm^3/g; Vex is the excess adsorption amount, cm^3/g; ρ_{a1}, ρ_{a2}, and ρ_a are the adsorbed phase densities of CH_4, CO_2, and binary gas, the values of ρ_{a1} and ρ_{a2} are approximately the reciprocal of the van der Waals volume, 0.372 g/cm^3 and 1.028 g/cm^3, respectively [50-51]; ρ_{g1}, ρ_{g2}, and ρ_g are the bulk phase density of CH_4, CO_2, and binary gas, the values are controlled by experimental temperature and pressure and calculated by NIST; x_1 and x_2 are the mole fractions of CH_4 and CO_2 in adsorbed phase; y_1 and y_2 are the mole fractions of CH_4 and CO_2 in bulk phase.

2.2.2 Fitting of adsorption data by Langmuir model

The Langmuir model (Eq. 4) is universally applied to the adsorption behavior of CH_4 and CO_2 in coal and shale matrix [52-53]. The application of the model is based on four assumptions, namely, (i) there is monolayer adsorption, (ii) the adsorption surface is uniform, (iii) there is no force among the adsorbed molecules, and (iv) the equilibrium of adsorption is a dynamic equilibrium [54]. The details and calculation equation are as follows:

$$Vabs = V_L P / (P / P_L) \tag{4}$$

V_L is the Langmuir volume, which represents the maximum adsorption amount when monolayer adsorption is saturated, cm^3/g. P_L is the Langmuir pressure, MPa, its value is the experimental pressure when the adsorption amount is $V_L/2$.

2.2.3 Selectivity coefficient calculation of CO_2 relative to CH_4

The adsorption amount of CO_2 on shale matrix is higher than CH_4, and Sc is used to quantitatively characterize the adsorption affinity of CO_2 relative to CH_4 in the binary gas adsorption system (Eq. 5) [55-56]. Upon reaching the adsorption equilibrium of each experimental pressure, the adsorption priority of CO_2 is stronger than CH_4 if Sc greater than 1, and the adsorption advantage of CO_2 increases with higher Sc.

$$Sc = (x_1/y_1)/(x_2/y_2) \tag{5}$$

Sc is the selectivity coefficient of CH_4 and CO_2 in the binary adsorption system, x_1 and y_1 are the mole fractions of CO_2 in an adsorbed phase and a bulk phase; x_2 and y_2 are the mole fractions of CH_4 in an adsorbed phase and a bulk phase.

3 Results and discussion

3.1 Absolute adsorption amounts of pure gas

Vabs of CH_4 and CO_2 is in the range of 0 - 2.86 cm^3/g and 0 - 17.69 cm^3/g, respectively. The adsorption amount of CO_2 is apparently higher than CH_4 under the same experimental conditions (Fig. 2), which is consistent with previous studies [16-17]. The shape of CH_4 and CO_2 adsorption isotherms is consistent with the characteristics of type I adsorption isotherm [57], also known as the Langmuir adsorption isotherm (Fig. 2). The Langmuir model (Eq. 4) presents a fairly high goodness of fit to CH_4 and CO_2 experimental data (R^2 = 0.996 and 0.978, respectively).

The adsorption ratio of CO_2 relative to CH_4 (AR) ranges from 3.842 to 6.210 (Fig. 3). AR and experimental pressure present a positive linear correlation (R^2 = 0.796) at 0 - 8 MPa. With further experimental pressure increase (10 - 20 MPa), AR stabilizes to an equilibrium value and does not increases anymore. In current literature, there is no unequivocal conclusion about the impact of pressure on AR. Zhou et al. [58] and Ghalandari et al. [59] stated that AR decreases with higher pressure, and the relative adsorption advantage of CO_2 decreases correspondingly. Ma et al. [20] stated that there is no significant linear correlation between AR and experimental pressure, AR initially decreases and then increases with higher experimental pressure. Additionally, results from Lee et al. [60] and Xie et al. [17] are similar to our finding with experimental pressure and AR exhibiting a positive linear correlation until an equilibrium value. The high adsorption amount and affinity of CO_2 relative to CH_4 are attributed to their molecular dynamics and thermodynamic properties [61-62], including the smaller molecule dynamic diameter, linear molecular configuration, higher boiling point and critical temperature, lower self-diffusion coefficient, and higher quadrupole moment and dipole moment of CO_2 [63-66]. The high internal energy and isosteric heat of adsorption of CO_2 also lead to a stronger adsorption than that of CH_4 [58,67-68].

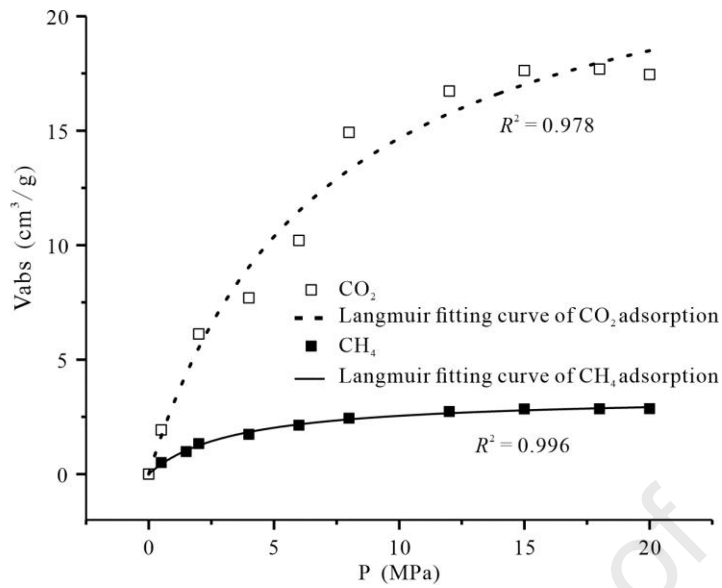

Vabs is the absolute adsorption amount of CO_2 and CH_4.

Fig. 2 Adsorption isotherms of CH_4 and CO_2 in sample XY-1

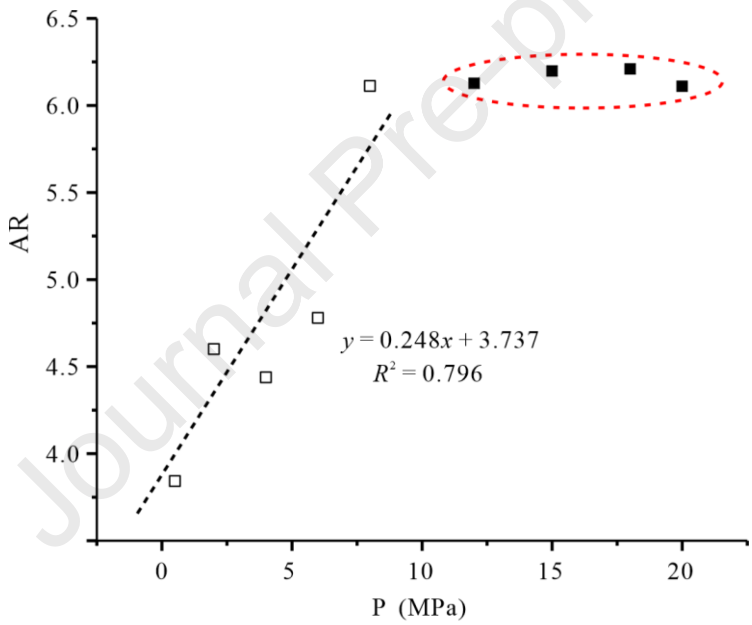

AR is adsorption ratio of CO_2 relative to CH_4 in pure gas adsorption experiments.

Fig. 3 Adsorption priority of CO_2 relative to CH_4 in sample XY-1

3.2 Binary gas adsorption behavior

3.2.1 Absolute adsorption amount of binary gas

The adsorption isotherms of binary gas are similar to pure CH_4 or CO_2 (Fig. 4), which are consistent with the characteristics of type I adsorption isotherm, and the Langmuir model also has better fitting results (R^2 = 0.9960, 0.9946, 0.9920, 0.9924, 0.9822, 0.9913, and 0.9782, respectively for the feed gas composition of CH_4 (100%), CH_4 (80%) + CO_2 (20%), CH_4 (60%) + CO_2 (40%), CH_4 (50%) + CO_2 (50%), CH_4 (40%) + CO_2 (60%), CH_4 (20%) + CO_2 (80%), and CO_2 (100%)). This indicates that the monolayer adsorption theory also applies to binary gas adsorption in a shale matrix. The adsorption amount of binary gas on shale is affected by the feed gas composition. V_L grows with higher CO_2 mole fraction in binary gas, and presents a positive linear correlation (R^2 =

0.985) (Fig. 5). This is in line with the general findings of other researchers, i.e. the adsorption amount of CO_2 in shale is greater than CH_4 and the increase in CO_2 mole fraction in the adsorption system increases the adsorption amount of binary gas accordingly [21,23].

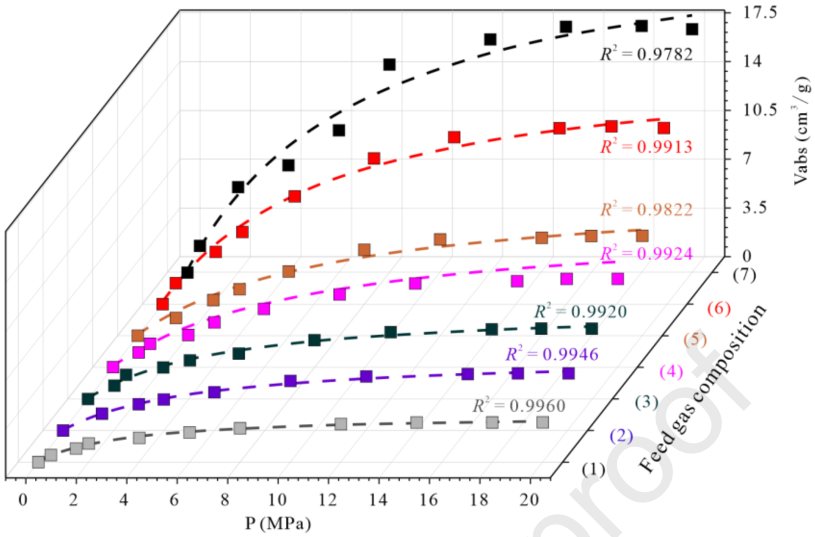

V_{abs} is the absolute adsorption amount of CH_4 and CO_2 in the binary adsorption system. (1) - (7) is the feed gases with the component of CH_4 (100%), CH_4 (80%) + CO_2 (20%), CH_4 (60%) + CO_2 (40%), CH_4 (50%) + CO_2 (50%), CH_4 (40%) + CO_2 (60%), CH_4 (20%) + CO_2 (80%), and CO_2 (100%).

Fig. 4 Vabs of binary gas on shale matrix of different feed gas composition in sample XY-1

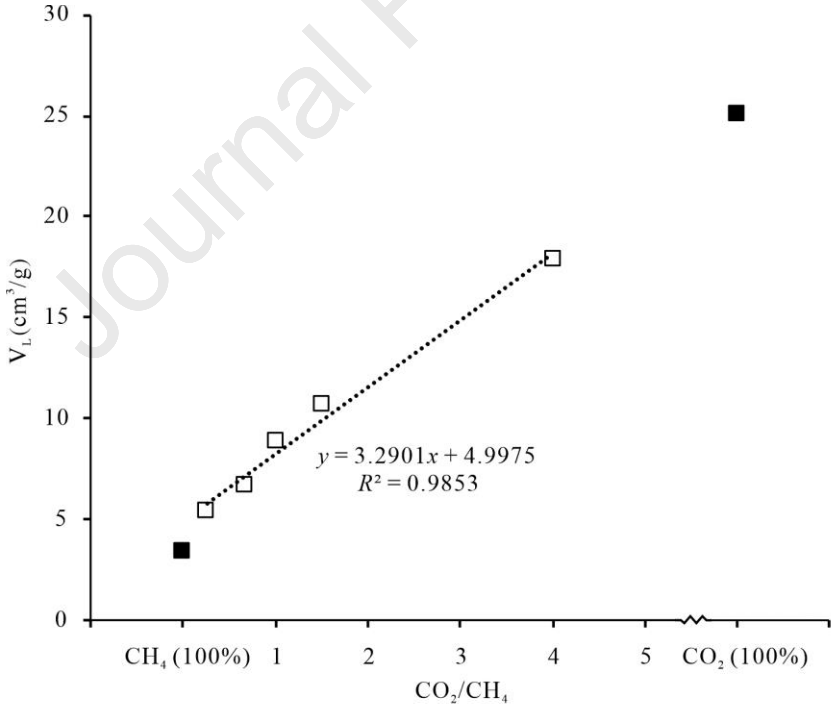

V_L is the Langmuir volume of CH_4 and CO_2 in the binary adsorption system.

Fig. 5 The correlation of V_L versus feed gas composition in sample XY-1

V_L of five shale samples is 6.63, 6.96, 6.28, 4.93, and 4.87 cm^3/g, respectively (Fig. 6). The influence of shale property (TOC and clay content) on V_L is investigated, and a positive linear correlation is observed between V_L and TOC (R^2 = 0.8769) (Fig. 7a). TOC represents the hydrocarbon generation potential; moreover, the pores in organic matter generated during hydrocarbon generation process is the essential enrichment space of shale gas [38,69-71]. V_L exhibits a weak negative linear correlation versus clay content (R^2 = 0.5517) (Fig. 7b). Furthermore, V_L is normalized by TOC to avoid the coupling effect of organic matter pores on shale gas adsorption capacity, and a positive linear correlation is found between normalized V_L (V_L/TOC) and clay content (R^2 = 0.6635) (Fig. 7c), which indicates that clay minerals generally improve the adsorption capacity of shale. However, the significance of the influence of clay is much lower than that of TOC, as the correlation can be affected by TOC, and even show a completely opposite trend (Fig. 7b and c).

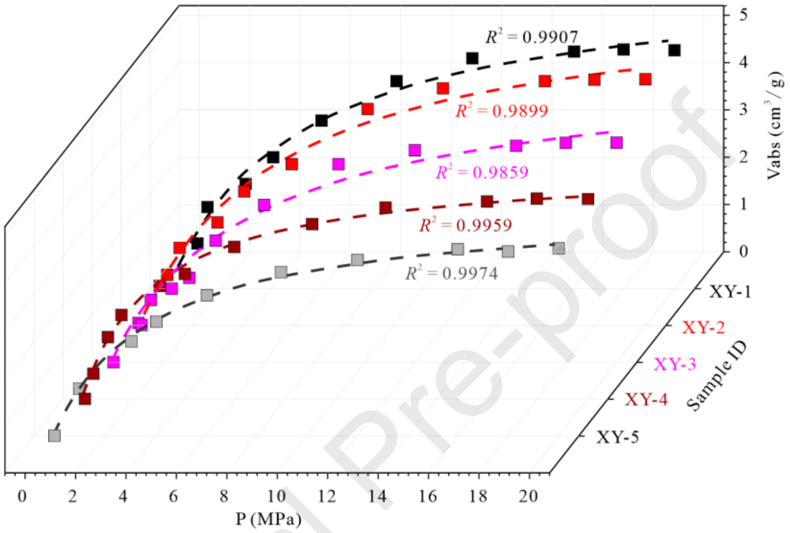

V_{abs} is the absolute adsorption amount of CH_4 and CO_2 in the binary adsorption system.

Fig. 6 Vabs of binary gas (CH_4 (60%) + CO_2 (40%)) adsorption in different shale samples

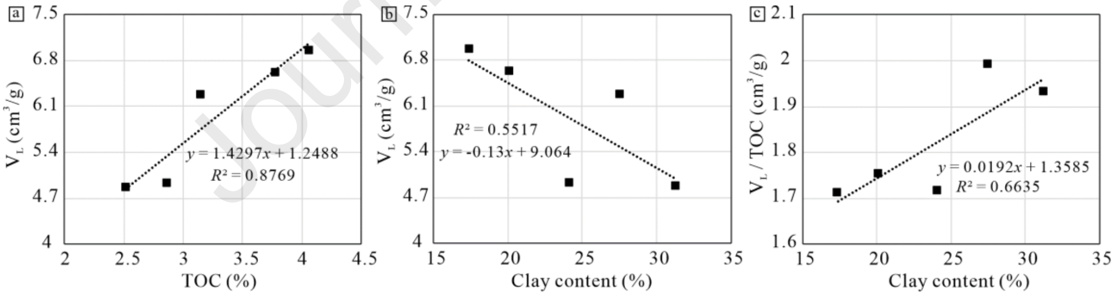

V_L is the Langmuir volume of CH_4 and CO_2 in the binary adsorption system. (a) is the correlation of V_L versus TOC, (b) is the correlation of V_L versus clay content, and (c) is the correlation of V_L/TOC versus clay content.

Fig. 7 The correlation of V_L versus TOC (a) and clay content (b and c)

3.2.2 Selectivity coefficient of CO_2 relative to CH_4

Sc of CO_2 and CH_4 adsorption on shale matrix is calculated using Eq. 5, and falls in the range of 4.58 - 5.65, 3.66 - 4.09, 3.19 - 3.61, 2.73 - 3.12, and 2.13 - 2.80 for the feed gas composition of CH_4 (80%) + CO_2 (20%), CH_4 (60%) + CO_2 (40%), CH_4 (50%) + CO_2 (50%), CH_4 (40%) + CO_2 (60%), and CH_4 (20%) + CO_2 (80%), respectively (Fig. 8). Sc decreases with higher experimental pressure, exhibiting an apparent negative exponential correlation (R^2 = 0.835, 0.983, 0.963, 0.897, and 0.956 for the five fitting lines, respectively) (Fig. 8). These finding are completely different from the above calculation results of AR value based on pure CO_2 and CH_4 adsorption results, which indicates that binary gas adsorption is different from pure component adsorption. The adsorption system is not only affected by the interaction between gas molecules and shale matrix, but also by the interaction among CH_4 and CO_2 molecules. A negative correlation or negative linear correlation of Sc versus experimental pressure has been observed in previous research [24,72]. However, the maximum experimental pressure (20 MPa) in our study is much higher than in previous experiments (mostly lower than 6 MPa). Sc stabilizes at an equilibrium value when the experimental pressure reaches 16 MPa, which implies that the influence of pressure on the selection coefficient is weaker than the feed gas composition in deep shale gas reservoirs. The correlation of Sc versus experimental pressure in different samples is similar to that of feed gas composition, showing a clear negative exponential correlation (R^2 = 0.983, 0.967, 0.970, 0.972, and 0.966 for the five shale samples, respectively) (Fig. 9).

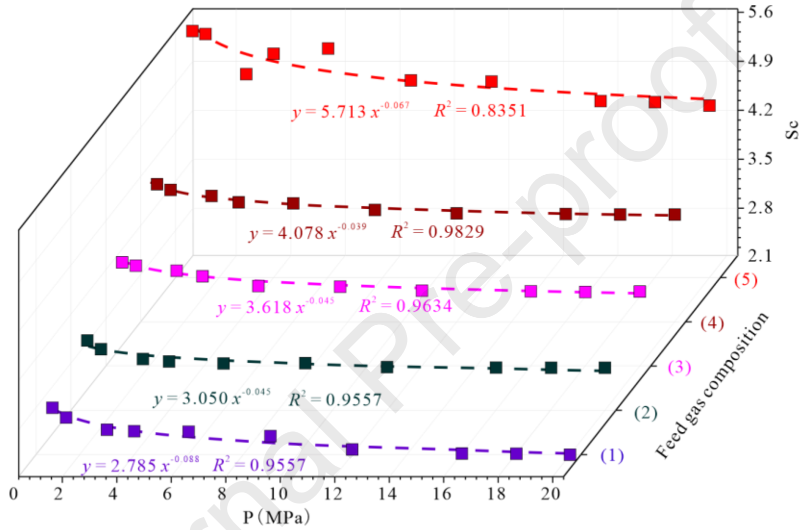

Sc is the selectivity coefficient of CH_4 and CO_2 in the binary adsorption system. (1) - (5) is the feed gases with the component of CH_4 (20%) + CO_2 (80%), CH_4 (40%) + CO_2 (60%), CH_4 (50%) + CO_2 (50%), CH_4 (60%) + CO_2 (40%), and CH_4 (80%) + CO_2 (20%).

Fig. 8 Selectivity coefficient of CH_4 and CO_2 adsorption under different feed gas ratio in sample XY-1

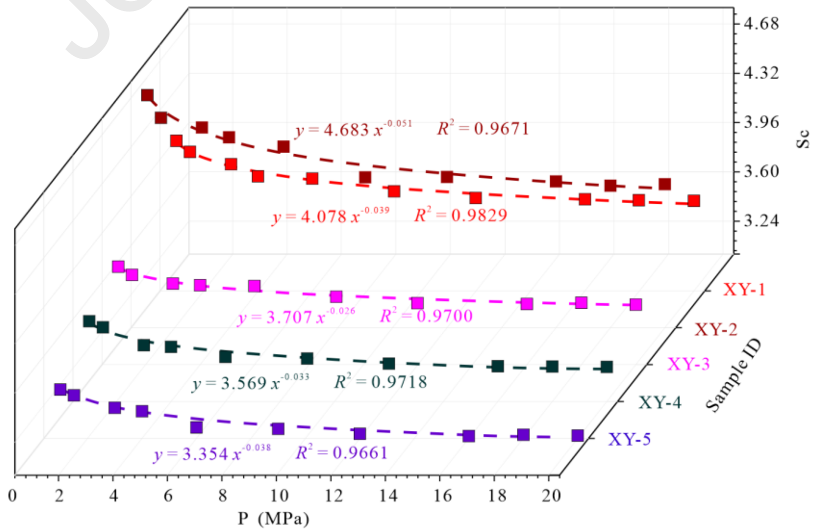

Sc is the selectivity coefficient of CH_4 and CO_2 in the binary adsorption system.

Fig. 9 Selectivity coefficient of CH_4 and CO_2 adsorption in the five shale samples (XY-1 - XY-5)

3.2.3 The influence of feed gas composition and shale property on Sc

Sc is a fundamental parameter and reference for the implementation of enhancing gas recovery (EGR) or CO_2 capture and storage (CCS) process. Hence, the influence of feed gas ratio and shale property (TOC, clay content, and pore structure parameters) on Sc are analyzed. Moreover, the application prospect of EGR or CCS process in different shale gas reservoirs is discussed.

(1) The influence of feed gas composition on Sc

As mentioned above, Sc stabilizes at an equilibrium value in high experimental pressure region (P > 16 MPa) in the competitive adsorption experiments with different feed gas composition or shale samples. Accordingly, Sc in 20 MPa of each experiment is selected as evaluation parameter for the adsorption affinity of CO_2 in high-pressure shale gas reservoir. Furthermore, a clear negative exponential correlation between Sc and the ratio of CO_2 and CH_4 in binary gas is found ($R^2 = 0.9929$) (Fig. 10). Hu et al. [73] reported similar molecular simulation results of CO_2 and CH_4 adsorption in montmorillonite and illite, and Zhang et al. [74] also observed a similar phenomenon in the competitive adsorption of CO_2 and CH_4 on coal matrix. However, there is no clear correlation between Sc and CO_2 ratio in Qin et al. [24]. The difference in their experimental/molecular simulation process is that Hu et al. [73] and Zhang et al. [74]'s simulation pressure is high (up to dozens MPa), the curves of Sc versus CO_2 ratio tend to be stable in the high-pressure stage, whereas Qin et al. [24]'s maximum experimental pressure is 6 MPa, hence the trend at high-pressure is not established. Overall, the lower proportion of CO_2 in feed gas would promote its utilization rate in the competitive adsorption process. Sc decreases continuously with higher CO_2 mole fraction, but the decrement is gradually getting smaller, which suggests that there is not only competitive adsorption between CH_4 and CO_2 molecules, but also among CO_2 molecules in the binary gas adsorption system. This phenomenon has opposing impacts on EGR or CCS processes in shale gas reservoirs. On the other hand, a low CO_2 ratio could improve CH_4 recovery and reduce economic cost on the premise of saving CO_2. A high CO_2 ratio is beneficial to the process of CO_2 geological sequestration. Therefore, the injection amount of CO_2 can be designed according to the shale gas resources in the gas-bearing basin, to achieve the main goal of enhancing either CH_4 recovery or CO_2 sequestration.

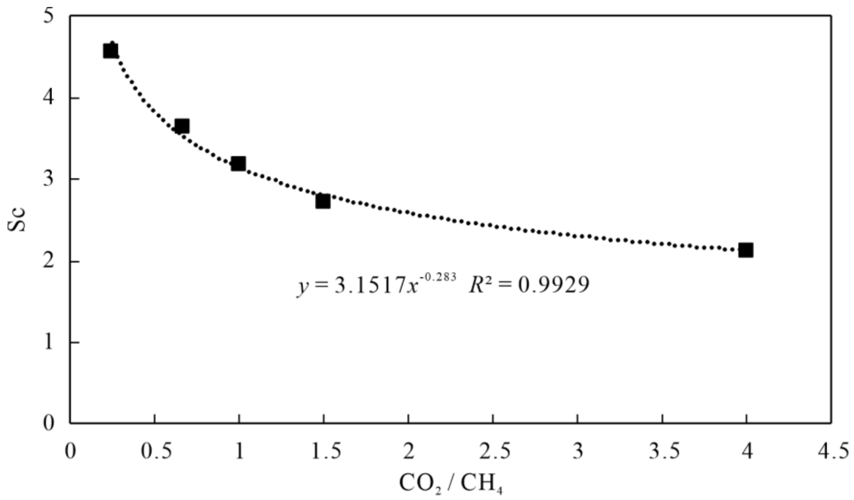

Sc is the selectivity coefficient of CH_4 and CO_2 in the binary adsorption system.

Fig. 10 The relationship of Sc versus CO_2/CH_4 in feed gas

(2) The influence of TOC and clay content on Sc

As presented in Fig. 11a and b, Sc exhibits a positive linear correlation versus TOC (R^2 = 0.9581) and a negative linear correlation versus clay content (R^2 = 0.8254). However, the Sc normalized by TOC and clay content shows a positive linear correlation (R^2 = 0.7954) (Fig. 11c). This phenomenon suggests that the strong adsorption capacity of shale is beneficial to improve CH_4 recovery after CO_2 injection. Sc shows a positive linear correlation versus clay content only after TOC normalization, which further proved that the clay content in the Longmaxi shale has a weak impact on the gas adsorption capacity and the adsorption affinity of CO_2 relative to CH_4. On the other hand, clay content in the Longmaxi shale is low (with an average content of 24.08%), and the content span in different samples is small (ranging from 17.39% to 27.54%). Hence, TOC should be taken as the major reference in the implementation of EGR or CCS process.

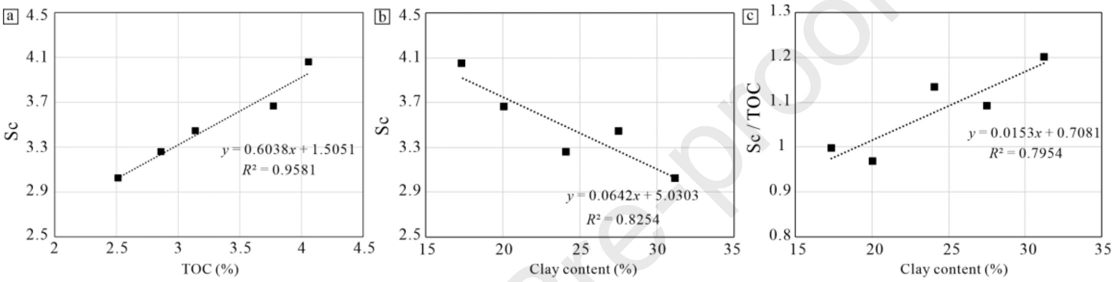

Sc is the selectivity coefficient of CH_4 and CO_2 in the binary adsorption system. (a) is the correlation of Sc versus TOC, (b) is the correlation of Sc versus clay content, and (c) is the correlation of Sc/TOC versus clay content.

Fig. 11 The relationship of Sc versus TOC and clay content

(3) The influence of pore structure parameters on Sc

CH_4 mainly occurs in the pores of shale gas reservoirs [75-76], and pore structure parameters are crucial controlling factors of the competitive adsorption behavior of CH_4 and CO_2 on shale matrix. The correlation of PV and SSA versus Sc are discussed, respectively. A positive linear correlation is manifested of pore volume (PV) with different pore sizes versus Sc, with decreasing goodness of fit (R^2) in the sequence of 0.9546 (0- 50 nm), 0.9544 (2 - 50 nm), 0.8816 (0 - 0.7 nm), 0.6149 (0 - 2 nm), 0.2011 (1.4 - 2 nm), and 0.0181 (0.7 - 1.4 nm) (Fig. 12a), which demonstrates that high PV is conducive to adsorption affinity of CO_2 relative to CH_4 in the shale matrix. The influence of mesopores on PV is greater than that of micropores, and the ultra-micropores dominate the PV of micropores, higher than middle-micropores and super-micropores, with the latter two contributing little to the pore volume and having a poor correlation with Sc (Fig. 12a). The contribution of micropores and mesopores to pore volume is different in shale reservoirs in different regions. Xie [77] reported that the contribution rate of micropores (44.83%) to PV is greater than that of mesopores (29.95%). In addition, Pang et al. [78] proved that the contribution of micropores and mesopores to pore volume varies in different shale samples.

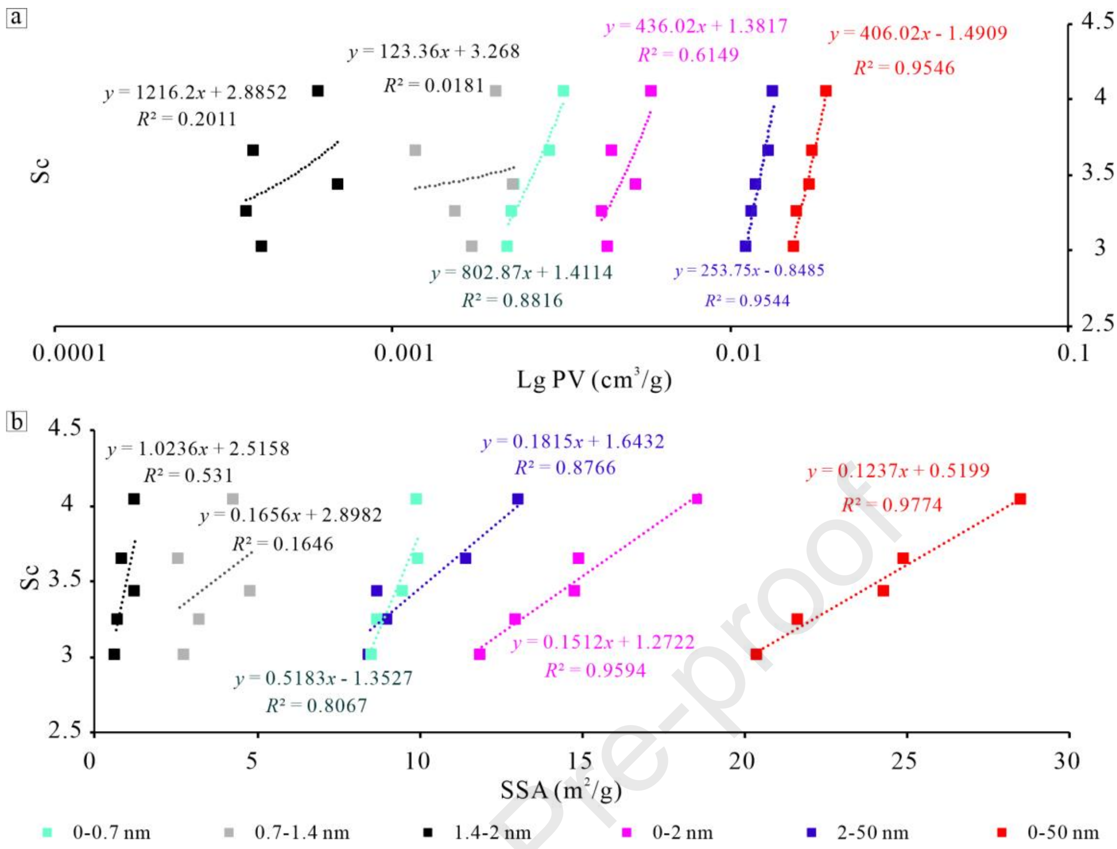

Sc is the selectivity coefficient of CH_4 and CO_2 in the binary adsorption system. "0 - 0.7 nm, 0.7 - 1.4 nm, 1.4 - 2 nm, 0 - 2 nm, 2 - 50 nm, and 0 - 50 nm" represents the pores with diameter in the range of 0 - 0.7 nm, 0.7 - 1.4 nm, 1.4 - 2 nm, 0 - 2 nm, 2 - 50 nm, and 0 - 50 nm, respectively.

Fig. 12 The relationship of Sc versus PV (a) and SSA (b) in different pore sizes

SSA with different pore sizes also has an apparent positive linear correlation versus Sc, and the degree of fit is better than PV (Fig. 12b). Similarly, R^2 of SSA with different pore sizes is obviously different, with the value is in the sequence of 0.9774 (0 - 50 nm), 0.9594 (0 - 2 nm), 0.8766 (0 - 0.7 nm), 0.8067 (2 - 50 nm), 0.531 (1.4 - 2 nm), and 0.1646 (0.7 - 1.4 nm). Micropores dominate SSA, even the contribution of ultra-micropores is higher than mesopores. The contribution of super-micropores and middle-micropores to SSA is much lower than ultra-micropores, and their correlation versus Sc is relatively unobtrusive, especially the latter. Micropores dominate SSA of Longmaxi shale, and researchers have reported similar conclusions [35-37]. In addition, our study also indicates that the PV and SSA of shale micropores are dominated by ultra-micropores, which also make a significant contribution to the adsorption capacity and Sc. Consequently, more attention should be paid to the study of ultra-micropores in future research on the pore structure characteristics of shale gas reservoirs.

(4) Relationship between TOC, clay content, pore structure parameters, adsorption capacity, and Sc

The influence of TOC on pore structure parameters and adsorption capacity of shale is primary, independently whether it concerns micropores, mesopores or macropores [79-80]. Inner pore of organic matter is the significant enrichment space of shale gas [69-70]. The influence of clay minerals on shale pore structure parameters and adsorption capacity is complex, and researchers have reported diverse results on different shale gas reservoirs. Ma et al. [81] stated that clay minerals have a significant contribution to pore structure parameters, which is reflected in a significant linear positive correlation, whereas the results of Xu et al. [82] exhibited a negative linear correlation, which is not conducive to the development of pore structure parameters. Additionally, Guo et al. [80] stated that the effect of clay content on pore structure parameters of shale is weak. Xie et al. [83] found that the correlation between clay minerals and pore structure parameters is controlled by the diagenetic evolution stages of shale. Clay content shows a good positive linear correlation versus PV and SSA of shale in early diagenetic and middle diagenetic stages, whereas there was no clear correlation in shale in the late mature stage [83]. Namely, interlayer water and interlayer pores of clay are discharged with further advanced diagenetic evolution, the porosity and pore number are much reduced, and the adsorption capacity and gas storage capacity are reduced accordingly. The Longmaxi shale gas reservoir is characterized as over mature, and the completion of smectite - illite transformation sequence is high, with an average illite content greater than 75%. Ji et al. [40] suggested that the adsorption capacity of illite is almost the lowest compared with other clay minerals. This is also a major reason for the weak influence of clay content on gas adsorption amount and Sc in our study.

In conclusion, there is a correlation between TOC, clay content, pore structure parameters, V_L, and Sc (Fig. 13). The main impact is TOC that dominates the development of micropores and mesopores in shale, which influences the development of PV and SSA, and further affects the adsorption capacity of shale and CO_2 adsorption affinity. Clay minerals contribute to some extent to mesopores, but their contribution is much lower than TOC, and it can only be detected after eliminating the influence of TOC. Additionally, we have also found that the micropores are mainly affected by ultra-micropores, and the contribution of middle-micropores and super-micropores is relatively lower. It remains to be verified in future research whether this phenomenon is universal in high-over maturity shale gas reservoirs.

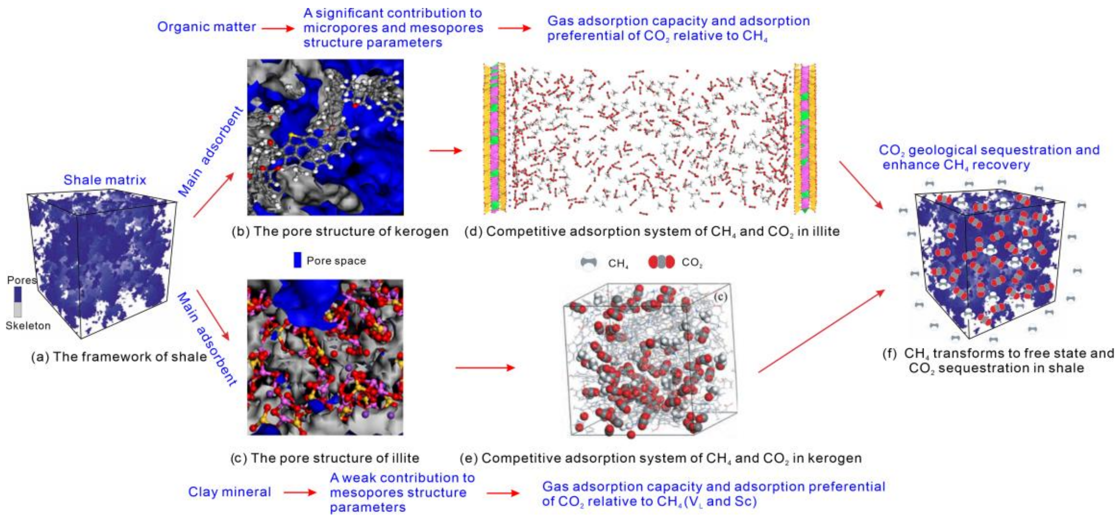

(a) is the three-dimension reconstruction of shale core based on nano-CT [84]; (b) and (c) are the pore structure model of kerogen and illite, respectively [30], the blue region is pore space; d is the molecular simulation process of the competitive adsorption behavior of CH_4 and CO_2 in illite [85]; (e) are the molecular simulation of CH_4 and CO_2 competitive in kerogen [86]; (f) is the ultimate-objective to realize CO_2 geological sequestration and enhance CH_4 recovery.

Fig. 13 Relationship between TOC, clay content, pore structure parameters, adsorption capacity, and Sc in molecular scale in shale matrix

Furthermore, experimental pressure and water content also influence the adsorption affinity of CO_2 relative to CH_4 in shale. Generally, high experimental temperature results in a decrease of the CO_2 adsorption capacity, and this decrease is larger than for CH4 adsorption capacity, which leads correspondingly to a drop in Sc [87-88]. On the other hand, the energy of gas molecules is greater at high temperature, and the energy barrier will be reduced at higher temperature. Therefore, gas can enter the pores more easily, especially CO_2 with a linear molecular structure and small molecular dynamics diameter [58,89]. The adsorption capacity of H_2O in shale is greater than that of CO_2 and CH_4, the pore throat and surface adsorption sites occupied by it lead directly to a reduction of gas adsorption capacity [90-92]. Furthermore, the effective pores of shale would be filled and separated into several smaller pores with a diameter less than the dynamic diameter of CO_2 and CH_4 [90-91]. The influence of water content on Sc is still debated. In the research of Wang et al. [55], water content has little effect on CO_2 adsorption affinity, and Sc fluctuates slightly with higher water content. However, Sui et al. [93] suggested that the presence of water molecules in shale kerogen have a greater impact on the adsorption capacity of CH_4 than that of CO_2. Also, other studies showed that when the water content further increases, the originally dispersed water molecules in the shale will regroup into clusters, and desorb from the oxygen-containing functional groups. Still, CO_2 occupies these adsorption sites again, thus Sc varies periodically with the change of water content [35,94]. The gas-liquid-solid mechanism of CO_2, CH_4, H_2O, and shale matrix still needs to be further explored. In addition, it should be noted that the effects of temperature and water content on CO_2 adsorption affinity in shale are mostly performed through molecular simulation. Due to the influence of structural accuracy, simulation condition, and pore structure characteristics of shale matrix, the results of molecular simulation are quite different, which still needs to be verified by matched experimental simulation.

3.3 The implication on CO_2 sequestration and enhanced CH_4 recovery

Currently, the burial depth of the exploited shale gas reservoir is in the range of 1000 - 6000 m, mostly less than 3500 m. Most of the high recovery reservoirs are overpressured with the corresponding reservoir pressure being much higher than the maximum experimental pressure (competitive adsorption experiments) under the current apparatus conditions. Therefore, to explore the CO_2 storage capacity at the conditions of real shale gas reservoirs and the potential to improve CH_4 recovery after CO_2 injection, mathematical models were established at reservoir conditions according to the main controlling factors of Sc in Chapter 3.2 (the fitting curves of Sc versus experimental pressure). Prediction of Sc is at different TOC and reservoir pressure. The calculated mathematical model is established from the fitting curves of Sc versus experimental pressure in different experimental shale samples. The details are as follows (Eqs. 6 - 11):

$$Sc_1 = 4.08*Pr\wedge{-0.0387} \tag{6}$$

$$Sc_2 = 4.68*Pr\wedge{-0.0512} \tag{7}$$

$$Sc_3 = 3.71*Pr\wedge{-0.0258} \tag{8}$$

$$Sc_4 = 3.57*Pr\wedge{-0.0334} \tag{9}$$

$$Sc_5 = 3.35*Pr\wedge{-0.0381} \tag{10}$$

Sc_1 - Sc_5 are Sc of different reservoir pressure corresponding to TOC of 3.78%, 4.065%, 3.15%, 2.87%, and 2.52%, respectively; Pr is reservoir pressure, MPa.

$$Pr = D \times Pc \tag{11}$$

D is the burial depth, km; Pc is pressure coefficient of the shale gas reservoir, its value is related to the burial depth and preservation conditions of the gas reservoir. In this work, the selection of Pc refers to the results of ref [77] on pressure coefficient at different burial depths and regions of the Longmaxi shale gas reservoir in the Changning area (sampling point of this work is located at the west edge of this area), southern Sichuan Basin.

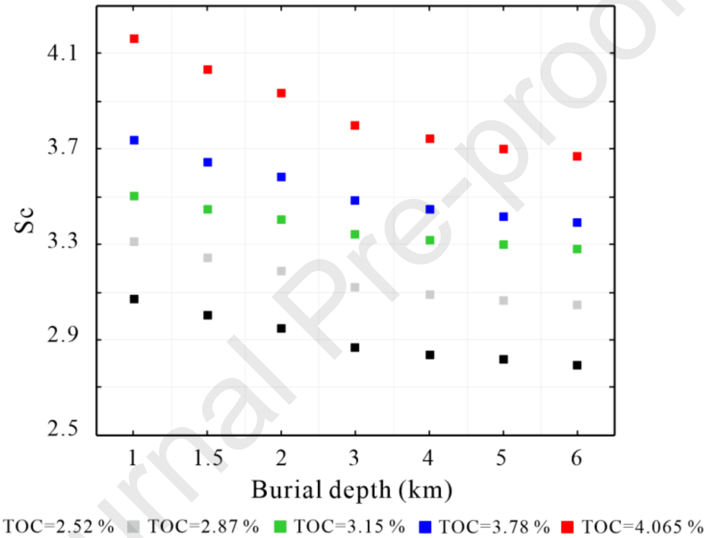

Sc is the selectivity coefficient of CH_4 and CO_2 in the binary adsorption system.

Fig. 14 The prediction results of Sc at different burial depth and TOC of the Longmaxi shale gas reservoirs, southern Sichuan Basin

Sc of five curves is in the range of 2.80 - 3.07, 3.04 - 3.31, 3.28 - 3.50, 3.39 - 3.73, and 3.66 - 4.16 in the prediction results (Fig. 14). The minimum value of Sc is 2.8 when the reservoir pressure depth reaches 6000 m (with a TOC value of 2.52). TOC has an apparent positive control on Sc, which implies that CO_2 injection into deep shale gas reservoir still has great potential for carbon storage and CH_4 recovery improvement, especially in organic-rich shale gas reservoirs. Additionally, a geological model of CO_2 geological sequestration and enhanced CH_4 recovery after CO_2 injection is established. CO_2 injection into shale gas reservoir is divided into three procedures (Fig. 15). (i) Supercritical CO_2 fracturing technology for shale gas reservoir, which has been successfully practiced and achieved promising effectiveness [95]. (ii) CO_2 competitive adsorbs with CH_4 to promote it desorption, and improves CH_4 recovery. (iii) CO_2 storage in the shale gas reservoir. Currently, (i) has been implemented in Ordos Basin, China and (ii) has been discussed above. Hence, we examine the CO_2 sealing capacity of the Longmaxi shale. Longmaxi shale is an unconventional reservoir with low porosity, low permeability, and strong self-sealing ability, which ensures the storage effect of CO_2 from the source. Baota Formation and Shiniulan Formation are the roof and floor of Longmaxi shale, which play an essential role in the sealing ability of gas reservoir, with the average porosity, average permeability, and average break through pressure are 1.5%, 0.013 mD, and 67.8 MPa, 0.59%, 0.0026 mD, and 76.1 MPa, respectively [96]. Additionally, Jialingjiang Formation of the Lower Triassic is a high-quality regional caprock, which also has a significant contribution to the sealing of gas, with a porosity lower than 10% and a permeability lower than 1 mD [97]. The basalt intrusion occurred during the Permian, and the Feixianguan Formation is characterized by a high porosity and permeability [98], so they are not regarded as high-quality regional caprocks (Fig. 15). Our experimental simulation verified the molecular simulation and numerical simulation results to some extent. Mohagheghian et al. [99] indicated that the adsorption capacity of CO_2 in shale is greater than CH_4, 30% - 55% of the injected CO_2 would be sealed in adsorption state in shale gas reservoirs. Moreover, this process improves CH_4 recovery by 8% - 16%. In addition, Mohagheghian et al. [99] suggested that the efficiency, safety, and application prospect of CO_2 stored in shale gas reservoirs are much better than that in deep saline aquifers. Liu et al. [100] also suggested that the CO_2 sealing ability of shale is excellent with a leakage risk lower than 1%.

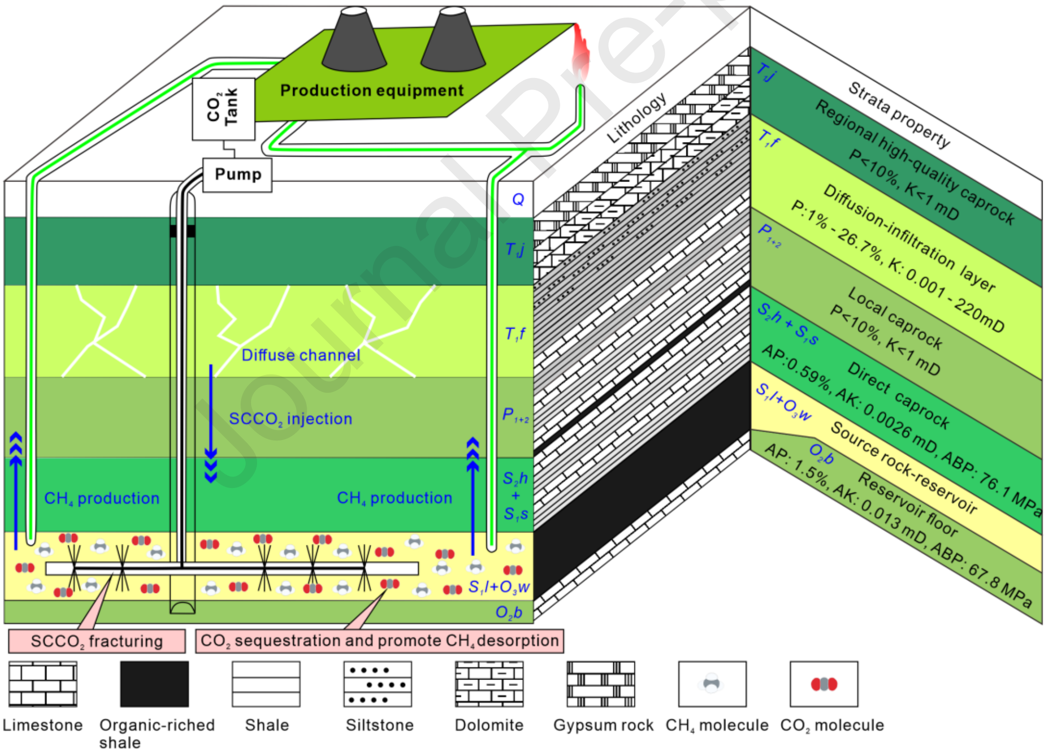

Q is the Quaternary, T_1j and T_1f are the Jialingjiang and Feixianguan Formations of Lower Triassic, P_{1+2} is the Lower-Middle Permian, S_2h is the Hanjiadian Formation of Middle Silurian, S_1s is the Shiniulan Formation of Lower Silurian, S_1l is the Longmaxi Formation of Lower Silurian, O_3w is the Wufeng Formation of Upper Ordovician, O_2b is the Baota Formation of Middle Ordovician. P is porosity, K is permeability, AP is the average porosity, AK is average permeability, ABP is average breakthrough pressure. The porosity, permeability, and breakthrough pressure refer to the results of ref [95-97,101].

Fig. 15 The geological model of CO_2 sequestration and enhancing CH_4 recovery in the Longmaxi Formation, southern Sichuan Basin

CO_2 injection into shale gas reservoir to store carbon and to improve CH_4 recovery has been proven to be theoretically feasible and it has great economic benefits. The optimal process is to stimulate the reservoir with supercritical CO_2 based fracturing fluid to increase production, displace the pre-adsorbed CH_4 to improve gas recovery, prolong the stable production cycle, and finally seal CO_2 in shale gas reservoirs [92]. Nevertheless, several critical bottlenecks hinder its application. CO_2 capture, purification, and transportation bring huge economic burden; The strong permeability and corrosivity of supercritical CO_2 require higher safety of storage and injection equipment and higher injection pressure, overpressure of ground equipment occurs frequently in pilot field tests; Sand carrying capacity of supercritical CO_2 is unfavorable caused by low viscosity, a high compatibility thickener is necessary; CO_2 injection amount, injection method, injection cycle, and stewing technique need more detailed demonstration; The interaction mechanism of CH_4-CO_2-H_2O-shale is extremely complex, which limits the research on the injectability of CO_2 and the competitive adsorption behavior of multicomponent gases in real shale reservoirs; Additionally, although researchers have discussed the safety of CO_2 storage in shale, the leakage risk cannot be ignored, a complete leakage monitoring system is also required after CO_2 injection, including atmospheric environment, groundwater resources, surface ecosystem, etc.

Conclusion

(1) The adsorption amount and affinity of CO_2 is greater than that of CH_4 in Longmaxi shale, the adsorption capacity of binary gas adsorption system increases with higher CO_2 mole fraction. The Langmuir model exhibits excellent fitting results for both pure gas adsorption and binary gas adsorption, and V_L increases with higher experimental pressure. Additionally, V_L is also influenced by organic matter content and mineralogical composition, there is a clear positive linear correlation between TOC and V_L. A negative linear correlation is observed between clay content and V_L affected by TOC, whereas a positive linear correlation is exhibited between clay content and V_L/TOC, which indicates that the impact of TOC is much higher than that of the clay content.

(2) The adsorption ratio of pure CO_2 and CH_4 is larger than the adsorption selectivity coefficient of CO_2 and CH_4 in binary gas adsorption system. There is a significant difference in the correlation between AR and Sc versus experimental pressure, the former depicts a linear correlation, whereas the latter exhibits a exponential correlation, which suggests that there is not only interaction between gas molecules and shale matrix, but also between CH_4 and CO_2 molecules. The adsorption affinity of CO_2 relative to CH_4 in shale is affected by TOC, clay content, adsorption capacity, and pore structure parameters. TOC and clay minerals control the pore structure of shale, the adsorption capacity of shale, and the adsorption affinity of CO_2 relative to CH_4.

(3) CO_2 injection into shale gas reservoirs has promising application prospects to improve CH_4 recovery and carbon emission reduction, even in overpressured reservoirs deeper than 6000 m. The geological conditions in the southern Sichuan Basin can ensure the sequestration safety after CO2 injection, as the Longmaxi shale is characterized by low porosity and permeability, which provides a good self-sealing ability. The underlying and overlying strata are also characterized by low porosity, low permeability, and high breakthrough pressure, forming an excellent lithologic trap. Additionally, the Jialingjiang Formation, composed of gypsum and dolomite, has a stable lithology

and strong sealing ability. It is an ideal regional high-quality caprock, and also plays a significant role in the geological sequestration of CO_2.

Acknowledgement

The authors gratefully acknowledge the support of the Fundamental Research Funds for National Universities, China University of Geosciences (Wuhan) [grant number: none] and the Major Project Cultivation of CUMT [grant number: 2020ZDPYMS09].

Author contribution

Experimental design and data analysis, Weidong Xie, Zhenghong Yu, and Hua Wang; writing and revision, Weidong Xie, Meng Wang, Si Chen, and Veerle Vandeginste.

Declaration of interest

The authors declare no conflict of interest.

Reference

[1] Liu H, Rao X, Xiong H. Evaluation of CO2 sequestration capacity in complex-boundary-shape shale gas reservoirs using projection-based embedded discrete fracture model (pEDFM)[J]. Fuel, 2020, 277: 118201.

[2] Huang L, Zhou W, Xu H, et al. Dynamic fluid states in organic-inorganic nanocomposite: implications for shale gas recovery and CO2 sequestration[J]. Chemical Engineering Journal, 2021, 411: 128423.

[3] Gholami R, Raza A, Andersen P, et al. Long-term integrity of shaly seals in CO2 geo-sequestration sites: An experimental study[J]. International Journal of Greenhouse Gas Control, 2021, 109: 103370.

[4] Pan Z, Connell L D. Reservoir simulation of free and adsorbed gas production from shale[J]. Journal of Natural Gas Science and Engineering, 2015, 22: 359-370.

[5] An M, Zhang F, Dontsov E, et al. Stress perturbation caused by multistage hydraulic fracturing: Implications for deep fault reactivation[J]. International Journal of Rock Mechanics and Mining Sciences, 2021, 141: 104704.

[6] Chailleux S, Merlin J, Gunzburger Y. Unconventional oil and gas in France: From popular distrust to politicization of the underground[J]. The extractive industries and society, 2018, 5(4): 682-690.

[7] Sampath K, Perera M S A, Ranjith P G, et al. CH4CO2 gas exchange and supercritical CO2 based hydraulic fracturing as CBM production-accelerating techniques: A review[J]. Journal of CO2 Utilization, 2017, 22: 212-230.

[8] Berardo R, Holm F, Heikkila T, et al. Hydraulic fracturing and political conflict: News media coverage of topics and themes across nine states[J]. Energy Research & Social Science, 2020, 70: 101660.

[9] Eshkalak, M. O.; Al-Shalabi, E. W.; Sanaei, A.; Aybar, U.; Kamy, S. "Enhanced Gas Recovery by CO2 Sequestration versus Re-fracturing Treatment in Unconventional Shale Gas Reservoirs." Paper presented at the Abu Dhabi International Petroleum Exhibition and Conference, Abu Dhabi, UAE, November 2014.

[10] Khosrokhavar, R.; Wolf, K. H.; Bruining, H. Sorption of CH4 and CO2 on a carboniferous shale from Belgium using a manometric setup. Int. J. Coal Geol. 2014, 128, 153-161.

[11] Sun F, Yao Y, Li G, et al. Simulation of real gas mixture transport through aqueous nanopores during the depressurization process considering stress sensitivity[J]. Journal of Petroleum Science and Engineering, 2019, 178: 829-837.

[12] Park S Y, Lee H S, Kim S, et al. Correlation between adsorbed methane concentration and pore structure of organic-rich black shale from the Liard Basin, Canada[J]. Journal of Natural Gas Science and Engineering, 2021: 104226.

[13] Bemani A, Baghban A, Mohammadi A H, et al. Estimation of adsorption capacity of CO2, CH4, and their binary mixtures in Quidam shale using LSSVM: Application in CO2 enhanced shale gas recovery and CO2 storage[J]. Journal of Natural Gas Science and Engineering, 2020, 76: 103204.

[14] Kim S, Santamarina J C. CO2 breakthrough and leak-sealing–Experiments on shale and cement[J]. International Journal of Greenhouse Gas Control, 2013, 19: 471-477.

[15] Lohr C D, Hackley P C. Using mercury injection pressure analyses to estimate sealing capacity of the Tuscaloosa marine shale in Mississippi, USA: Implications for carbon dioxide sequestration[J]. International Journal of Greenhouse Gas Control, 2018, 78: 375-387.

[16] Cancino O P O, Pérez D P, Pozo M, et al. Adsorption of pure CO2 and a CO2/CH4 mixture on a black shale sample: Manometry and microcalorimetry measurements[J]. Journal of Petroleum Science and Engineering, 2017, 159: 307-313.

[17] Xie W, Wang M, Wang H. Adsorption Characteristics of CH4 and CO2 in Shale at High Pressure and Temperature[J]. ACS omega, 2021, 6(28): 18527-18536.

[18] Sun F, Yao Y, Li G, et al. Transport behaviors of real gas mixture through nanopores of shale reservoir[J]. Journal of Petroleum Science and Engineering, 2019, 177: 1134-1141.

[19] Sun F, Yao Y, Li G, et al. A slip-flow model for multi-component shale gas transport in organic nanopores[J]. Arabian Journal of Geosciences, 2019, 12(5): 1-11.

[20] Ma Y, Yue C, Li S, et al. Study of CH4 and CO2 competitive adsorption on shale in Yibin, Sichuan Province of China[J]. Carbon Resources Conversion, 2019, 2(1): 35-42.

[21] Sun J, Chen C, Hu W, et al. Asymmetric competitive adsorption of CO2/CH4 binary mixture in shale matrix with heterogeneous surfaces[J]. Chemical Engineering Journal, 2021, 422: 130025.

[22] Zhao G, Wang C. Influence of CO2 on the adsorption of CH4 on shale using low-field nuclear magnetic resonance technique[J]. Fuel, 2019, 238: 51-58.

[23] Du X, Cheng Y, Liu Z, et al. Study on the adsorption of CH4, CO2 and various CH4/CO2 mixture gases on shale[J]. AEJ - Alexandria Engineering Journal, 2020, 59(6), 5165-5178.

[24] Qin C, Jiang Y, Zhou J, et al. Effect of supercritical CO2 extraction on CO2/CH4 competitive adsorption in Yanchang shale[J]. Chemical Engineering Journal, 2021, 412: 128701.

[25] Dong D, Shi Z, Guan Q, et al. Progress, challenges and prospects of shale gas exploration in the Wufeng–Longmaxi reservoirs in the Sichuan Basin[J]. Natural Gas Industry B, 2018, 5(5): 415-424.

[26] Fan C, Li H, Qin Q, et al. Geological conditions and exploration potential of shale gas reservoir in Wufeng and Longmaxi Formation of southeastern Sichuan Basin, China[J]. Journal of Petroleum Science and Engineering, 2020, 191: 107138.

[27] Ge X, Hu W, Ma Y, et al. Quantitative evaluation of geological conditions for shale gas preservation based on vertical and lateral constraints in the Songkan area, Northern Guizhou, southern China[J]. Marine and Petroleum Geology, 2021, 124: 104787.

[28] Wang X, Zhai Z, Jin X, et al. Molecular simulation of CO2/CH4 competitive adsorption in organic matter pores in shale under certain geological conditions[J]. Petroleum Exploration and Development, 2016, 43(5): 841-848.

[29] Iddphonce R, Wang J. Investigation of CO2 and CH4 competitive adsorption during enhanced shale gas production[J]. Journal of Petroleum Science and Engineering, 2021, 205: 108802.

[30] Babatunde K A, Negash B M, Mojid M R, et al. Molecular simulation study of CO2/CH4 adsorption on realistic heterogeneous shale surfaces[J]. Applied Surface Science, 2021, 543: 148789.

[31] Ren W, Tian S, Li G, et al. Modeling of mixed-gas adsorption on shale using hPC-SAFT-MPTA[J]. Fuel, 2017, 210: 535-544.

[32] Liu B, Qi C, Mai T, et al. Competitive adsorption and diffusion of CH4/CO2 binary mixture within shale organic nanochannels[J]. Journal of Natural Gas Science and Engineering, 2018, 53: 329-336.

[33] Rouquerol J, Avnir D, Fairbridge C W, et al. Physical chemistry division commission on colloid and surface chemistry, subcommittee on characterization of porous solids: recommendations for the characterization of porous solids[J]. Pure and Applied Chemistry, 1994, 66(8): 1739-1758.

[34] Xie W, Chen S, Vandeginste V, et al. Review of the Effect of Diagenetic Evolution of Shale Reservoir on the

Pore Structure and Adsorption Capacity of Clay Minerals[J]. Energy & Fuels, 2022. https://doi.org/10.1021/acs.energyfuels.2c00675

[35] Wang Y, Liu L, Zheng S, et al. Full-scale pore structure and its controlling factors of the Wufeng-Longmaxi shale, southern Sichuan Basin, China: Implications for pore evolution of highly overmature marine shale[J]. Journal of Natural Gas Science and Engineering, 2019, 67: 134-146.

[36] Lyu C, Zhang Y, Li C, et al. Pore characterization of Upper Ordovician Wufeng Formation and Lower Silurian Longmaxi Formation shale gas reservoirs, Sichuan Basin, China[J]. Journal of Natural Gas Geoscience, 2020, 5(6):327-340.

[37] Wang X, Liu L, Wang Y, et al. Comparison of the pore structures of Lower Silurian Longmaxi Formation shales with different lithofacies in the southern Sichuan Basin, China[J]. Journal of Natural Gas Science and Engineering, 2020, 81: 103419.

[38] Zhu H, Ju Y, Huang C, et al. Microcosmic gas adsorption mechanism on clay-organic nanocomposites in a marine shale[J]. Energy, 2020, 197: 117256.

[39] Zhang J, Tang Y, He D, et al. Full-scale nanopore system and fractal characteristics of clay-rich lacustrine shale combining FE-SEM, nano-CT, gas adsorption and mercury intrusion porosimetry[J]. Applied Clay Science, 2020, 196: 105758.

[40] Ji L, Zhang T, Milliken K, et al. Experimental investigation of main controls to methane adsorption in clay-rich rocks[J]. Applied Geochemistry, 2012, 27(12):2533-2545.

[41] Lin Y, Wang S, Sha Y, et al. Organic geochemical characteristics of bark coal in Changguang area: evidence from aromatic hydrocarbons[J]. International Journal of Coal Science & Technology, 2020, 7(2): 288-298.

[42] Zhang X, Xue G, Bao J, et al. Research on fat coal quality difference[C]//2011 International Conference on Materials for Renewable Energy & Environment. IEEE, 2011, 2: 1711-1714.

[43] Fan C, Zhong C, Zhang Y, et al. Geological Factors Controlling the Accumulation and High Yield of Marine‐Facies Shale Gas: Case Study of the Wufeng‐Longmaxi Formation in the Dingshan Area of Southeast Sichuan, China[J]. Acta Geologica Sinica‐English Edition, 2019, 93(3): 536-560.

[44] Zhang P, Lu S, Li J, et al. Characterization of shale pore system: a case study of Paleogene Xin'gouzui Formation in the Jianghan basin, China[J]. Marine and Petroleum Geology, 2017, 79: 321-334.

[45] Tian H, Pan J, Zhu D, et al. Innovative one-step preparation of activated carbon from low-rank coals activated with oxidized pellets[J]. Journal of Cleaner Production, 2021, 313: 127877.

[46] Pang W, Jin Z. Ono-Kondo lattice model for propane multilayer adsorption in organic nanopores in relation to shale gas[J]. Fuel, 2019, 235: 158-166.

[47] Ghasemzadeh H, Babaei S, Tesson S, et al. From excess to absolute adsorption isotherm: The effect of the adsorbed density[J]. Chemical Engineering Journal, 2021, 425: 131495.

[48] Chen L, Liu K, Jiang S, et al. Effect of adsorbed phase density on the correction of methane excess adsorption to absolute adsorption in shale[J]. Chemical Engineering Journal, 2021, 420: 127678.

[49] Huang X, Gu L, Li S, et al. Absolute adsorption of light hydrocarbons on organic-rich shale: An efficient determination method[J]. Fuel, 2022, 308: 121998.

[50] Sircar S. Gibbsian surface excess for gas adsorption revisited[J]. Industrial & engineering chemistry research, 1999, 38(10): 3670-3682.

[51] Rexer T F T, Benham M J, Aplin A C, et al. Methane adsorption on shale under simulated geological temperature and pressure conditions[J]. Energy & Fuels, 2013, 27(6): 3099-3109.

[52] Ye Z, Chen D, Pan Z, et al. An improved Langmuir model for evaluating methane adsorption capacity in shale under various pressures and temperatures[J]. Journal of Natural Gas Science and Engineering, 2016, 31: 658-680.

[53] Tang X, Ripepi N, Stadie N P, et al. A dual-site Langmuir equation for accurate estimation of high pressure deep shale gas resources[J]. Fuel, 2016, 185: 10-17.

[54] Langmuir I. The constitution and fundamental properties of solids and liquids. Journal of the Franklin institute. 1917, 102-105, 0016-0032.

[55] Wang T, Tian S, Li G, et al. Molecular simulation of CO2/CH4 competitive adsorption on shale kerogen for CO2 sequestration and enhanced gas recovery[J]. The Journal of Physical Chemistry C, 2018, 122(30): 17009-17018.

[56] Zhou W, Wang H, Zhang Z, et al. Molecular simulation of CO2/CH4/H2O competitive adsorption and diffusion in brown coal[J]. RSC advances, 2019, 9(6): 3004-3011.

[57] IUPAC. 1972. In physisorption, van der waals forces are accompanied by electrostatic forces that has the ability to hold more than one monomolecular layers.

[58] Zhou W, Wang H, Yan Y, et al. Adsorption mechanism of CO2/CH4 in kaolinite clay: insight from molecular simulation[J]. Energy & Fuels, 2019, 33(7): 6542-6551.

[59] Ghalandari V, Hashemipour H, Bagheri H. Experimental and modeling investigation of adsorption equilibrium of CH4, CO2, and N2 on activated carbon and prediction of multi-component adsorption equilibrium[J]. Fluid Phase Equilibria, 2020, 508: 112433.

[60] Lee S P, Mellon N, Shariff A M, et al. High-pressure CO2-CH4 selective adsorption on covalent organic polymer[J]. Journal of Natural Gas Science and Engineering, 2018, 50: 139-146.

[61] Song X, Ma X, Zeng Y. Adsorption equilibrium and thermodynamics of CO2 and CH4 on carbon molecular sieves[J]. Applied Surface Science, 2017, 396: 870-878.

[62] Rocha L A M, Andreassen K A, Grande C A. Separation of CO2/CH4 using carbon molecular sieve (CMS) at low and high pressure[J]. Chemical Engineering Science, 2017, 164: 148-157.

[63] Reznik A, Aingh P, Foi E. An Analysis of the Effect of CO2 Injection on the Recovery of Insitu Methane from Bituminous Coal: An Experimental Simulation[J]. SPE Journal, 1984, 24 (5):521-528.

[64] Clarkson C, Bustin R. Binary Gas Adsorption/Desorption Isotherms: Effect of Moisture and Coal Composition upon Carbon Dioxide Selectivity over Methane[J]. International Journal of Coal Geology, 2000, 42 (4):241-272.

[65] Link A N, Link J R. National Institute of Standards and Technology[M]. Springer US, 2006.

[66] Panicker P, Magid A. Microwave plasma gasification for enhanced oil recovery and sustainable waste management[C]//ASME 2016 10th International Conference on Energy Sustainability collocated with the ASME 2016 Power Conference and the ASME 2016 14th International Conference on Fuel Cell Science, Engineering and Technology. American Society of Mechanical Engineers Digital Collection, 2016.

[67] Myers A L. Thermodynamics of adsorption in porous materials[J]. AIChE Journal, 2002, 48(1): 145-160.

[68] Duan S, Gu M, Tao M, et al. Adsorption of methane on shale: statistical physics model and site energy distribution studies[J]. Energy & Fuels, 2019, 34(1): 304-318.

[69] Romero-Sarmiento M F, Rouzaud J N, Bernard S, et al. Evolution of Barnett Shale organic carbon structure and nanostructure with increasing maturation[J]. Organic Geochemistry, 2014, 71: 7-16.

[70] Löhr S C, Baruch E T, Hall P A, et al. Is organic pore development in gas shales influenced by the primary porosity and structure of thermally immature organic matter?[J]. Organic Geochemistry, 2015, 87: 119-132.

[71] Jiang W, Cao G, Luo C, et al. A composition-based model for methane adsorption of overmature shales in Wufeng and Longmaxi Formation, Sichuan Basin[J]. Chemical Engineering Journal, 2021: 130766.

[72] Huo P, Zhang D, Yang Z, et al. CO2 geological sequestration: displacement behavior of shale gas methane by carbon dioxide injection[J]. International Journal of Greenhouse Gas Control, 2017, 66: 48-59.

[73] Hu X, Deng H, Lu C, et al. Characterization of CO2/CH4 competitive adsorption in various clay minerals in relation to shale gas recovery from molecular simulation[J]. Energy & Fuels, 2019, 33(9): 8202-8214.

[74] Zhang J, Liu K, Clennell M B, et al. Molecular simulation of CO2–CH4 competitive adsorption and induced coal swelling[J]. Fuel, 2015, 160: 309-317.

[75] Zou J, Rezaee R, Liu K. Effect of temperature on methane adsorption in shale gas reservoirs[J]. Energy & Fuels,

2017, 31(11): 12081-12092.

[76] Xie W, Wang M, Duan H. Adsorption Characteristics and Controlling Factors of CH4 on Coal-Measure Shale, Hedong Coalfield[J]. Minerals, 2021, 11(1): 63.

[77] Xie W. Reservoir Characteristics and Gas Preservation of the Longmaxi Formation in the Changning Area, South Sichuan [D]. China University o Shale f Mining and Technology, Xuzhou, 2020.

[78] Pang P, Han H, Hu L, et al. The calculations of pore structure parameters from gas adsorption experiments of shales: Which models are better?[J]. Journal of Natural Gas Science and Engineering, 2021(4):104060.

[79] Zhu H, Zhang T, Liang X, et al. Insight into the pore structure of Wufeng-Longmaxi black shales in the south Sichuan Basin, China[J]. Journal of Petroleum Science and Engineering, 2018, 171: 1279-1291.

[80] Guo X, Qin Z, Yang R, et al. Comparison of pore systems of clay-rich and silica-rich gas shales in the lower Silurian Longmaxi formation from the Jiaoshiba area in the eastern Sichuan Basin, China[J]. Marine and Petroleum Geology, 2019, 101: 265-280.

[81] Ma X, Guo S, Shi D, et al. Investigation of pore structure and fractal characteristics of marine-continental transitional shales from Longtan Formation using MICP, gas adsorption, and NMR (Guizhou, China)[J]. Marine and Petroleum Geology, 2019, 107:555-571.

[82] Xu Z, Shi W, Zhai G, et al. Study on the characterization of pore structure and main controlling factors of pore development in gas shale[J]. Journal of Natural Gas Geoscience, 2020, 5(5): 255-271.

[83] Xie W, Wang M, Wang H, et al. Diagenesis of shale and its control on pore structure, a case study from typical marine, transitional and continental shales[J]. Frontiers of Earth Science, 2021: 1-17.

[84] Pang W. Reconstruction of digital shale cores using multi-point geostatistics[J]. Natural Gas Industry, 2017, 37(09):71-78.

[85] Chong L, Myshakin E M. Molecular simulations of competitive adsorption of carbon dioxide–methane mixture on illitic clay surfaces[J]. Fluid Phase Equilibria, 2018, 472: 185-195.

[86] Sui H, Yao J. The CO2/CH4 Competitive Adsorption in Kerogen: A Molecular Simulation [J]. Science Technology and Engineering, 2017, 16(11): 128-131.

[87] Pan Z, Ye J, Zhou F, et al. CO2 storage in coal to enhance coalbed methane recovery: a review of field experiments in China[J]. International Geology Review, 2018, 60(5-6): 754-776.

[88] Lee H, Shakib F A, Shokouhimehr M, et al. Optimal separation of CO2/CH4/Brine with amorphous Kerogen: A thermodynamics and kinetics study[J]. The Journal of Physical Chemistry C, 2019, 123(34): 20877-20883.

[89] Liu J, Xi S, Chapman W G. Competitive sorption of CO2 with gas mixtures in nanoporous shale for enhanced gas recovery from density functional theory[J]. Langmuir, 2019, 35(24): 8144-8158.

[90] Gensterblum Y, Merkel A, Busch A, et al. High-pressure CH4 and CO2 sorption isotherms as a function of coal maturity and the influence of moisture[J]. International Journal of Coal Geology, 2013, 118: 45-57.

[91] Huang L, Ning Z, Wang Q, et al. Molecular simulation of adsorption behaviors of methane, carbon dioxide and their mixtures on kerogen: Effect of kerogen maturity and moisture content[J]. Fuel, 2018, 211: 159-172.

[92] Xie W, Chen S, Wang M, et al. Progress and Prospects of Supercritical CO2 Application in the Exploitation of Shale Gas Reservoirs[J]. Energy & Fuels, 2021, 35(22): 18370-18384.

[93] Sui H, Zhang F, Wang Z, et al. Effect of kerogen maturity, water content for carbon dioxide, methane, and their mixture adsorption and diffusion in kerogen: a computational investigation[J]. Langmuir, 2020, 36(33): 9756-9769.

[94] Huang L, Ning Z, Wang Q, et al. Effect of organic type and moisture on CO2/CH4 competitive adsorption in kerogen with implications for CO2 sequestration and enhanced CH4 recovery[J]. Applied Energy, 2018, 210: 28-43.

[95] Wang H, Li G, Zheng Y, et al. Research status and prospects of supercritical CO2 fracturing technology [J]. Acta Petrolei Sinica, 2020, 41 (1), 116-126.

[96] He S, Qin Q, Fan C, et al. Shale gas preservation conditions in Dingshan area, Southeastern Sichuan[J].

Petroleum Geology and Recovery Efficiency, 2019, 26(2):24-31.
[97] Wang S, Peng Y, Xiao G, et al. Sedimentary facies and reservoir characteristics of Jialingjiang formation in Puguang area[J], Petroleum Geology and Engineering, 2021, 35(1): 8-14, 21.
[98] Ou F, Yang H. Application of logging interpretation method for reef shoal reservoir in Feixianguan Formation of Gas Field X[J]. Petroleum Reservoir Evaluation and Development, 2021, 11(05):744-752.
[99] Mohagheghian E, Hassanzadeh H, Chen Z. CO2 sequestration coupled with enhanced gas recovery in shale gas reservoirs[J]. Journal of CO2 Utilization, 2019, 34: 646-655.
[100] Liu F, Ellett K, Xiao Y, et al. Assessing the feasibility of CO2 storage in the New Albany Shale (Devonian–Mississippian) with potential enhanced gas recovery using reservoir simulation. Int. J. Greenhouse Gas Control, 2013, 17, 111-126.
[101] Ning C. Reservoir characteristics and favorable area prediction of Qixia Formation in Shuangyushi area, North Sichuan[D]. Chengdu, Chengdu University of Technology, 2020.

Highlights

1. Adsorption affinity is controlled by feed gas composition and shale property.

2. Sc are coupling affected by TOC, clay content, and pore structure parameters.

3. Ultra-micropores dominate pore volume and specific surface area of micropores.

4. EGR-CCS has a promising application prospect.

Declaration of interests

☒ The authors declare that they have no known competing financial interests or personal relationships that could have appeared to influence the work reported in this paper.

☐The authors declare the following financial interests/personal relationships which may be considered as potential competing interests: